

PERFORMANCE STUDY OF CONICAL STRIP INSERTS IN TUBE HEAT EXCHANGER USING WATER BASED TITANIUM OXIDE NANOFLUID

by

Mahalingam ARULPRAKASAJOTHI^{a*,}, Kariappan ELANGO VAN^b,
Udayagiri CHANDRASEKHAR^{a***}, and Sivan SURESH^c**

^a Department of Mechanical Engineering, Veltech Dr. RR & Dr. SR Technical University,
Chennai, Tamil Nadu, India

^b Department of Mechanical Engineering, Cambridge Institute of Technology, Bangalore,
Karnataka, India

^c Department of Mechanical Engineering, National Institute of Technology, Trichy, Tamil Nadu, India

Original scientific paper
<https://doi.org/10.2298/TSCI151024250A>

The objective of the study is to observe the Nusselt number and friction factor behavior in a tube heat exchanger fitted with staggered and non-staggered conical strip inserts using water based titanium oxide nanofluid under laminar flow conditions. Water based titanium oxide nanofluid was prepared using a two-step method with a volume concentration of 0.1% and 0.5%. The tube inserts used were staggered and non-staggered conical strips having three different twist ratios of 2, 3, and 5. The experimental results indicated that the Nusselt number increased in the presence of water based titanium oxide nanofluid compared to the base fluid. Nusselt number further increased enormously with the use of conical strip inserts than a tube with no inserts. It was observed that the strip geometry and the nanofluid had a major effect on the thermal performance of the circular tube heat exchanger. It was found that with the staggered conical strip having a twist ratio of $Y = 3$ and 0.5% volume concentration of nanofluid provided the highest heat transfer. Correlations have been derived using regression analysis.

Key words: Nusselt number, friction factor, titanium oxide nanofluid, conical strip

Introduction

Improvisation of the performance of the heat exchanger has wide range of applications [1]. Heat exchangers play a significant role in internal combustion engines, air conditioning, various power plant, and all energy related areas [2]. In this, one of the techniques is to produce a working fluid with increased properties by using modern technology [3]. Remarkable developments in the field of nanotechnology provide an opportunity to produce new working fluid called nanofluid for thermal equipment. Initially, it was prepared by Choi [4] with different volume concentrations. Lee *et al.* [5] measured the thermal property of nanofluids and compared it with the base fluid. The result shows a positive effect thermal conductivity over the negative effect of increase in viscosity. Advantages of nanofluids are high specific area, high dispersion stability, and adjustable properties [6].

* Corresponding author, e-mail: mapj08@gmail.com

** Now at: Vel Tech Rangarajan Dr. Sagunthala R&D Institute of Science and Technology, Avadi, Chennai, Tamil Nadu, India

*** Now at: Department of Aeronautical Engineering, Vel Tech Rangarajan Dr. Sagunthala R&D Institute of Science and Technology, Avadi, Chennai, Tamil Nadu, India

Recent review articles from Haddad *et al.* [7] and Sidik *et al.* [8] illustrated the preparation methods of nanofluids. Choi *et al.* [9] initiated the heat transfer study with property measurements. Utomo *et al.* [10] showed that thermal conductivity of titanium oxide is lower than Maxwell model and viscosity is higher than Einstein-Bachelor model. Chandrasekar and Suresh [11] studied the mechanisms of Heat transport in nanofluids.

The heat transfer rate increased due to the addition of nanoparticles without any flow passage [12]. Sajadi *et al.* [13] reported that heat transfer coefficient increases by 11% and 18% with increasing volume fractions of ZnO-water nanofluid, respectively, to 1 vol.% and 2 vol.%. Shanthi *et al.* [14] studied the heat transfer character of nanofluids with improved thermal transport properties. The swirl flow devices are a passive method that has independent power property [15].

Some of the swirl flow devices are Helical screw tapes, wire coil inserts with geometrical considerations were used in tube exchangers. Karimi *et al.* [16] proposed new empirical correlation to predict the viscosity of nanofluids as a function of volume concentration, temperature, and the viscosity of base fluid.

Sundar and Manoj [17] reviewed the effect of different inserts. Chandrasekar *et al.* [18] found that the heat transfer enhances 34% with the use Al_2O_3 nanofluids and further increases was observed up to 20% with wire coil inserts along with Al_2O_3 nanofluids. Selvaraj *et al.* [19] analyzed different geometry of grooved tube like circular, square and trapezoidal using CFD. Selvam *et al.* [20] reported twisted tape with pins are desirable in order to increase the heat transfer rate. Suresh *et al.* [21] observed enhancement observed 48% enhancement in Nusselt number using spiral rod insert. Chandrasekar *et al.* [22] experimental result shows the Al_2O_3 nanofluids increase the Nusselt number up to 12.24% due to the effect of wire coil inserts. Shahidi *et al.* [23] investigated heat transfer and pressure drop behavior of MWCNT-water nanofluid turbulent flow inside vertical coiled wire inserted tubes and observed 102% increase in Nusselt number. This paper presents both the convective heat transfer and friction factor characteristics in the fully developed laminar flow using TiO_2 -water nanofluid with 0.1 %vol. and 0.5 %vol. concentration under constant heat flux with staggered and non-staggered conical strip inserts.

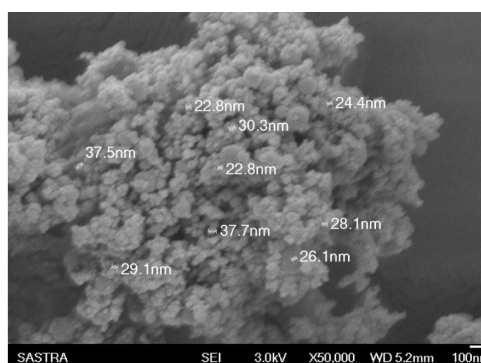


Figure 1. The SEM analysis of TiO_2 nanoparticles

Preparation of nanofluids

Water-based TiO_2 nanofluids was prepared with concentrations of 0.1%, and 0.5% using two step method. Nanofluid with an essential volume concentration was prepared by dispersing measured quantities of TiO_2 nanoparticles in distilled water. After dispersion the fluid were sonicated in an ultrasonic bath continuously for six hours to develop a uniform dispersion and stable suspension which govern the final properties of nanofluids [24]. Diameter of nanoparticles are verified using SEM analysis. Figure 1 shows the surface morphology of TiO_2 nanoparticles.

Thermophysical properties of TiO_2 -water nanofluid

The thermal conductivity of TiO_2 -water nanofluid was measured using a KD₂ pro thermal analyzer. The experimental value of thermal conductivity was compared with Maxwell's equation [25]. Maxwell proposed this model for spherical nanoparticles.

$$\frac{k_{nf}}{k} = \frac{k_s + 2k + 2\Phi(k_s - k)}{k_s + 2k - 2\Phi(k_s - k)} \quad (1)$$

From the correlation proposed by Yu and Choi [26] is given by eq. (2):

$$k_{nf} = \frac{1}{4}[(3\Phi - 1)k_s + (2 - 3\Phi)k] + \frac{k}{4}\sqrt{\Delta} \quad (2)$$

where

$$\Delta = \left[(3\Phi - 1)^2 \left(\frac{k_s}{k} \right)^2 + (2 - 3\Phi)^2 + 2(2 + 9\Phi - 9\Phi^2) \left(\frac{k_s}{k} \right) \right]$$

where k_{nf} is the thermal conductivity of nanofluid, k_s – the thermal conductivity of solid particle, k – the thermal conductivity of bulk fluid, and Φ – the volume fraction.

Figure 2 shows the comparison of experimental data with Maxwell and Choi classical models. The results show reasonably good agreement with the classical models at the lower concentration, however the experimental value were found to deviate from the classical models at higher concentrations.

The viscosity of nanofluid was measured by Brookfield cone and plate viscometer. The viscosities of TiO₂-water nanofluid were measured for different particle concentrations using Brookfield viscometer. Figure 3 shows the comparison of viscosities of the experimental values with theoretical values based on models proposed by Einstein, eq. (3), Batchelor, eq. (4), and Brinkman, eq. (5) models [27]:

$$\text{Einstein model} \quad \mu_{nf} = \mu(1 + k_1\Phi) \quad (3)$$

$$\text{Batchelor model} \quad \eta_{nf} = \mu(1 + k_1\Phi + k_2\Phi^2) \quad (4)$$

$$\text{Brinkman model} \quad \mu_{nf} = \frac{\mu}{(1 - \Phi)^{3/2}} \quad (5)$$

where μ_{nf} is the viscosity of nanofluid and μ – the viscosity of base fluid.

The stability of the nanofluid at different concentrations were measured by measuring the zeta potential. It was ensured that the nanoparticles were dispersed well and the nanofluid was stable due to very large repulsive forces between the nanoparticles as the pH is far from isoelectric point [28].

Table 1 shows the level of stability with respect to the zeta potential values. From the data obtained from the tab. 1, we can conclude from the fig. 4, that the TiO₂ nanofluid is stable.

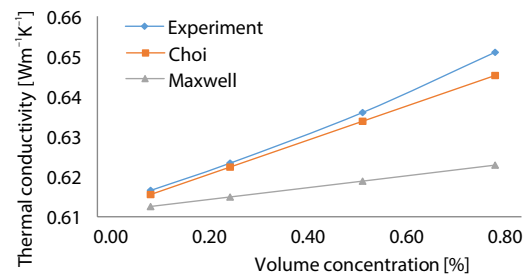


Figure 2. Experimental value of thermal conductivity of TiO₂-water nanofluids compared to classical models

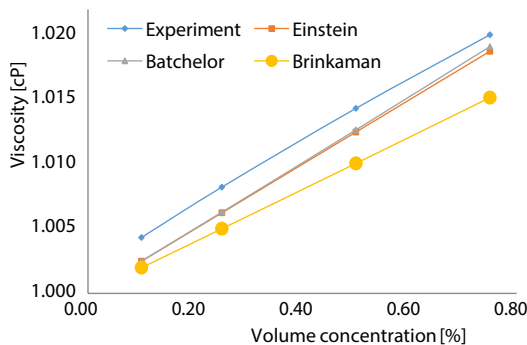
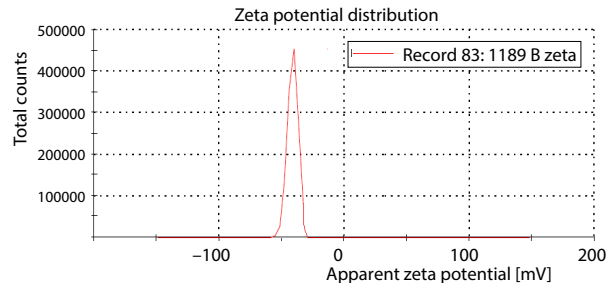
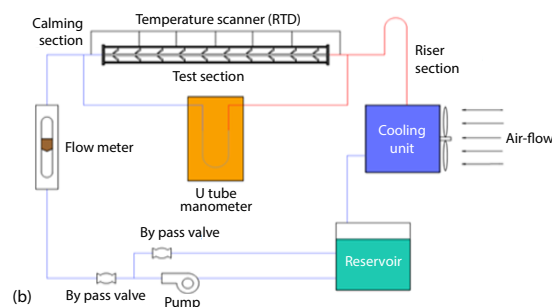
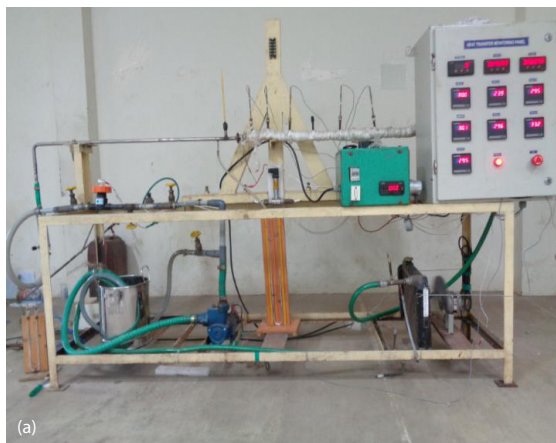


Figure 3. Comparison of viscosities of the experimental values with theoretical values

Table 1. Stability of nanofluids for different zeta potential values

Zeta potential, [mV]	Stability behavior of the colloid
0 to ± 5	Rapid coagulation or flocculation
± 10 to ± 30	Incipient instability
± 30 to ± 40	Moderate stability
± 40 to ± 60	Good stability
more than ± 61	Excellent stability

**Figure 4. Zeta potential values for TiO₂-water nanofluids****Figure 5. (a) Photographic view of set-up, (b) schematic diagram of set-up****Table 2. Twist ratios used in the experiment**

Pitch length [mm]	Diameter [mm]	Twist ratio Y
20	10	2:1
30	10	3:1
50	10	5:1

uniformly connected over the entire length of the rod. On the contrary, non-staggered conical strips are those which are randomly distributed over the entire length of the rod. The strips are

Experimental set-up and operating procedure

Figure 5(a) shows the photographic view of the experimental set-up. The set-up consisted of a calming section, test section, riser section, reservoir and pumping. The nanofluid is stored in a reservoir and pumped from the reservoir by a circulating pump. The nanofluid enters the calming section, this section serves to smooth the flow prior to entry into test section. The test section is made of a Cu tube of 1 m length and having an internal diameter of 0.01 m. Figure 5(b) shows the schematic diagram of set-up.

The heat flux is applied to the test section by an insulated nichrome heating wire having a capacity of 300 W. To reduce the heat loss to the atmosphere the heater wound test section is insulated by glass wool. Temperatures along the wall of the test section were measured by seven RTD which have an accuracy of ± 0.1 °C. Following the test section is the riser section. The riser section aids in maintaining a uniform flow in the test section and also to run full. The pressure drop along the test section is measured by a mercury U-Tube manometer. The fluid flow is measured by a rotameter. Figure 6(a) shows the staggered and non-staggered conical strip inserts. Staggered conical strips are those which are uni-

made of Cu sheet having 1 mm thickness. The geometry of the conical strip defined in fig. 6(b). The twist ratio equation and the different twist ratios used in the experiment are, tab. 2:

Y = pitch length of the rod / diameter of the test section

Data reduction

The friction factor for fully developed flow was determined by Poiseuille equation:

$$f = \left(\frac{D_i}{L} \right) \left(\frac{2\Delta P}{\rho u_m^2} \right) \quad (6)$$

Change in pressure was calculated using U-tube manometry where mercury is used as manometry fluid. The heat transfer rate was calculated by:

$$Q = \frac{V^2}{R} = \dot{m} C_p (T_{\text{out}} - T_{\text{in}}) = hA(T_w - T_{f,\text{avg}}) \quad (7)$$

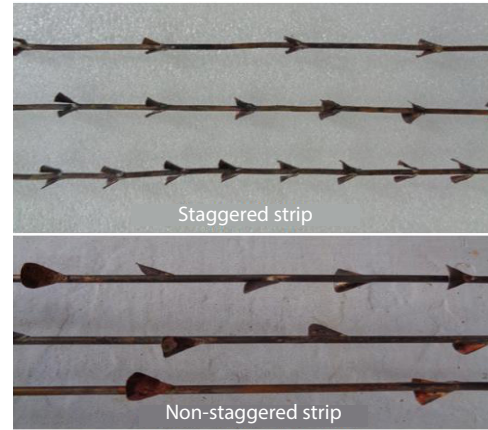


Figure 6(a). Different types of strips

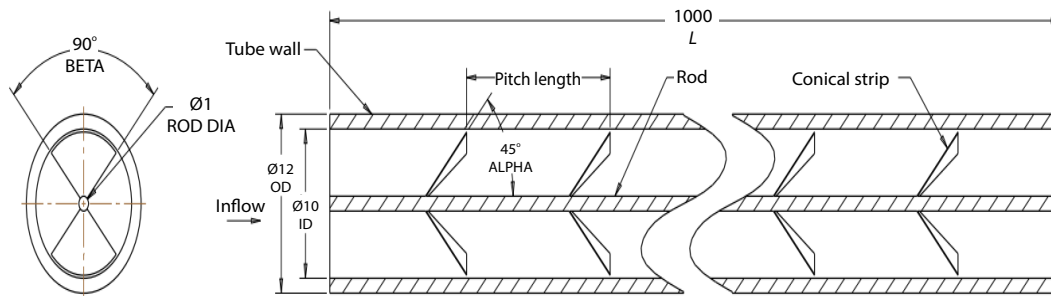


Figure 6(b). Geometry of the conical strip (OD – outside and ID – inside diameter)

The Nusselt number was calculated using eq. (8):

$$Nu = \frac{hD}{k} \quad (8)$$

Results and discussion

Initially, the experiment was conducted on a tube with no inserts for validation. The experimental Nusselt number data was verified by comparing the results with Shah equation for laminar flow. Figure 7 shows the comparison of Nusselt number for experimental and theoretical data.

Shah equation for laminar flow:

$$Nu = 1.953 \left(\text{RePr} \frac{D}{L} \right)^{1/2} \quad (9)$$

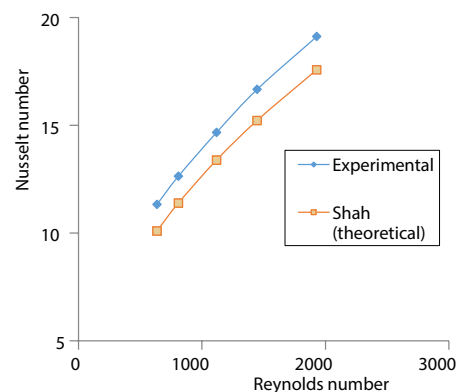


Figure 7. Nusselt number vs. Reynolds number for experimental and theoretical data

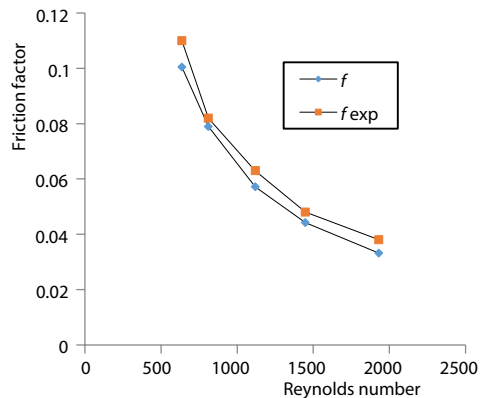


Figure 8. Friction factor verification

It can be seen that the maximum rate of Nusselt number was obtained for nanofluid with 0.5% concentration and having a twist ratio of 3. These results indicate that for a given Reynolds number, the increase in Nusselt number with increase in volume concentration is not same always. Level of flow turbulence made by separation and reattachment mechanism using conical strips. The chaotic movement of the solid particles in the flow will disturb the thermal boundary-layer formation at the surface of the tube wall. This disturbance would delay the development of thermal boundary-layer. Due to this higher heat transfer coefficient of the fluid was observed. Figure 10 shows that the friction factors of nanofluids at various Reynolds numbers. There was a moderate increase with the increase in friction factor due to conical strip inserts.

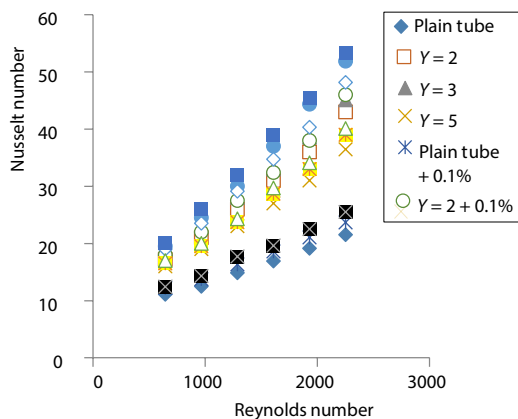


Figure 9. Nusselt number observation for staggered conical strip

Poiseuille equation:

$$f = \left(\frac{D_t}{L} \right) \left(\frac{2\Delta P}{\rho u_m^2} \right) \quad (10)$$

Similarly, the friction factor comparison was made with the Poiseuille eq. (10). Figure 8 shows the comparison of experimental friction factor with theoretical results. The figure shows that the experiment results are in good agreement with the theoretical results

Figure 9 represents the Nusselt number vs. Reynolds number under laminar flow conditions with staggered tape inserts. The maximum Nusselt number was achieved with the use of conical strip inserts as compared to plain tube.

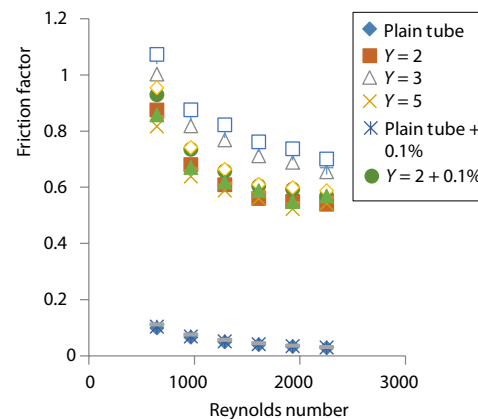


Figure 10. Friction factor observation for staggered conical strip

Figure 11 represents the Nusselt number vs. Reynolds number under laminar flow conditions with non-staggered tape inserts. It can be seen that the maximum rate of Nusselt number was obtained for nanofluid with 0.5 %vol. and having a twist ratio of fig. 12 shows that the friction factors of nanofluids at various Reynolds numbers. There was a moderate increase with the increase in friction factor due to conical strip inserts.

Nanofluid enhances the heat transfer rate as compared to regular coolants. Moreover, the use of inserts further increases the tube enhancement capabilities. Conical strip insert allows

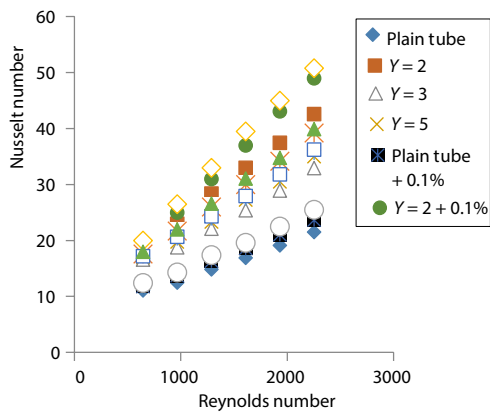


Figure 11. Nusselt number observation for non-staggered conical strip

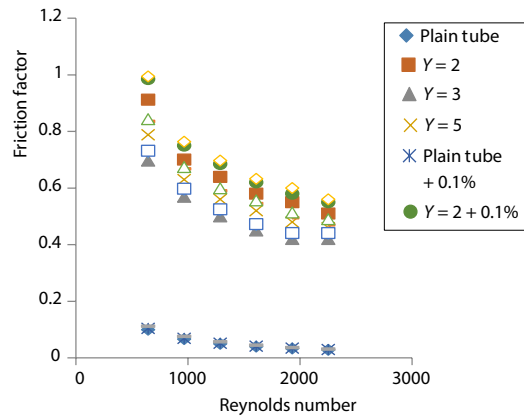


Figure 12. Friction factor observation for non-staggered conical strip

a greater mixing of fluid inside the heat exchanger tube and increases the turbulence in the tube. It promotes higher shear stress on the wall, which in turn promoted the heat transfer from the tube wall to the core as reflected by temperature field.

The addition of inserts in the tube has led to the requirement of higher pumping power. A balance has to be made considering the economics with respect to the increased pumping power requirement and the heat transfer with the conical inserts.

In this study, based on the experimental data, correlations were developed by using regression analysis for determining Nusselt number and friction factor with TiO_2 -water nanofluids. This correlation is developed for conical strip inserts.

$$\text{Nu} = 0.0169\text{Re}^{0.721}\text{Pr}^{1.637}Y^{-1.164}(1+\Phi)^{0.2328} \quad (11)$$

$$f = 0.7764\text{Re}^{-0.350}\text{Pr}^{1.686}Y^{-0.081}(1+\Phi)^{0.1384} \quad (12)$$

The previous equations, the Nusselt number and friction factor is a function of Reynolds number, Prandtl number, twist ratio, and nanofluid volume concentration. From figs. 13 and 14, it can be seen that the eqs. (11) and (12) are in agreement with the experimental values.

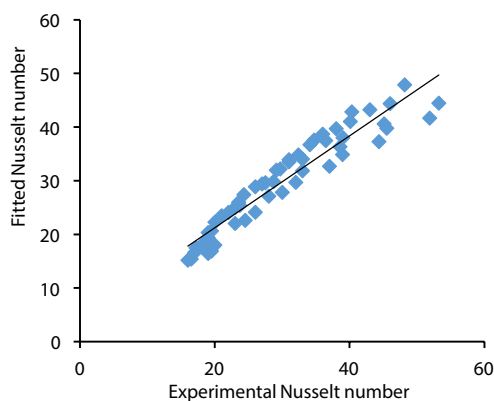


Figure 13. Comparison of experimental and fitted Nusselt number

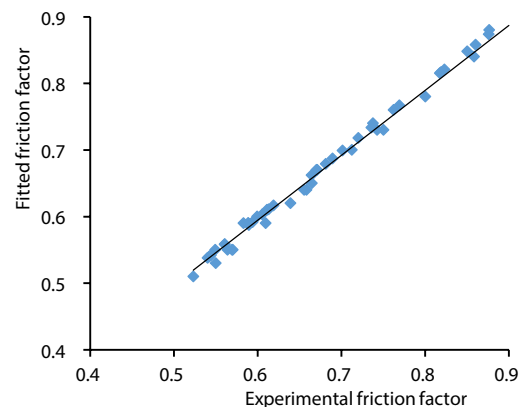


Figure 14. Comparison of experimental and fitted friction factor

Conclusions

In this study the Nusselt number and friction factor characteristics of water based TiO_2 nanofluids were analyzed. The experiment was carried out in a tube heat exchanger fitted with Staggered and non-staggered types of conical strips having three different twist ratios of 2, 3, and 5 under laminar flow conditions. The following observations were made as follows.

- The nanofluid showed increased heat transfer on comparison with base fluid alone, thereby enhancing the heat transfer capabilities of regular fluid.
- The use of staggered and non-staggered conical inserts was found to further increase the Nusselt number.
- The maximum Nusselt number was achieved at Reynolds number of 2251 with 0.5 %vol. when staggered conical strips were used with a twist ratio of 3.
- In case of non-staggered conical strips, the maximum Nusselt number was observed for a lower twist ratio of 2 having the same concentration of 0.5% of nanofluid, and
- The conical inserts increased the friction factor of the flow. This in turn increases the pumping power requirements. A balance has to be achieved considering the heat transfer improvement requirement and pumping power availability.

Nomenclature

A	– surface area of the tube, [m ²]	Q	– heat transfer, [W]
C_p	– specific heat, [Jkg ⁻¹ K ⁻¹]	R	– resistance, [Ω]
D	– diameter of the tube, [m]	Re	– Reynolds number
f	– friction factor	T_f	– fluid temperature, [°C]
h	– heat transfer coefficient, [Wm ⁻² K ⁻¹]	T_w	– wall temperature, [°C]
k_{nf}	– thermal conductivity of nanofluid, [Wm ⁻¹ K ⁻¹]	V	– voltage, [V]
k_s	– thermal conductivity of solid, [Wm ⁻¹ K ⁻¹]	U	– overall heat transfer coefficient, [Wm ⁻² K ⁻¹]
L	– length of the test section, [m]	u	– mean velocity, [ms ⁻¹]
\dot{m}	– mass flow rate, [kgs ⁻¹]	Y	– twist ratio
Nu	– Nusselt number	Greek symbols	
Pr	– Prandtl number	ρ	– density, [kgm ⁻³]
Δp	– pressure drop, [Nm ⁻²]	Φ	– volume fraction

References

- [1] Choi, S. U. S., Nanofluids: A New Field of Scientific Research and Innovative Applications, *Heat Transfer Engineering*, 29 (2008), 5, pp. 429-431
- [2] Arulprakasajothi, M., *et al.*, Convective Heat Transfer Characteristics of Nanofluids, *Proceedings, Frontiers in Automobile and Mechanical Engineering*, IEEE, Chennai, India, 2010, pp. 201-204
- [3] Koblinski, P., *et al.*, Mechanism of Heat Flow in Suspensions of Nano-Sized Particles (nanofluids), *International Journal of Heat and mass transfer*, 45 (2002), 4, pp. 855-863
- [4] Choi, S. U. S., Developments and Applications of Non-Newtonian Flows, *Proceedings, ASME FED*, San Francisco, Cal., USA, Vol. 66, 1995, pp. 99-105
- [5] Lee, S., *et al.*, Measuring Thermal Conductivity of Fluids Containing Oxide Nanoparticles, *ASME*, 121 (1999), 2, pp. 280-290
- [6] Arulprakasajothi, M., *et al.*, Experimental Study of Preparation, Characterisation and Thermal Behaviour of Water-Based Nanofluids Containing Titanium Oxide Nanoparticles, *Applied Mechanics & Materials*, 766-767 (2015), June, pp. 348-354
- [7] Haddad, Z., *et al.*, A Review on How the Researchers Prepare their Nanofluids, *International Journal of Thermal Sciences*, 76 (2014), Feb., pp. 168-189
- [8] Sidik, N. A. C., *et al.*, A Review on Preparation Methods and Challenges of Nanofluids, *International Communications in Heat and Mass Transfer*, 54 (2014), May, pp. 115-125
- [9] Choi, S. U. S., *et al.*, Anomalous Thermal Conductivity Enhancement in Nanotube Suspensions, *Applied Physics Letters*, 79, (2001), 14, pp. 2252-2254

- [10] Utomo, A. T., *et al.*, Experimental and Theoretical Studies of Thermal Conductivity, Viscosity and Heat Transfer Coefficient of Titania and Alumina Nanofluids, *International Journal of Heat and Mass Transfer*, 55 (2012), 25-26, pp. 7772-7781
- [11] Chandrasekar, V., Suresh, S., A Review on the Mechanisms of Heat Transport in Nanofluids, *Heat Transfer Engineering*, 30 (2009), 14, pp. 1136-1150
- [12] Arulprakasajothi, M., *et al.*, Heat Transfer Study of Water-Based Nanofluids Containing Titanium Oxide Nanoparticles, *Materials Today: Proceedings*, 2 (2015), 4-5, pp. 3648-3655
- [13] Sajadi, A. R., *et al.*, Experimental Study on Turbulent Heat Transfer, Pressure Drop, and Thermal Performance of ZnO/Water Nanofluid Flow in a Circular Tube, *Thermal Science*, 18 (2014), 4, pp. 1315-1326
- [14] Shanthi, R., *et al.*, Heat Transfer Enhancement Using Nanofluids an Overview, *Thermal Science*, 16 (2012), 2, pp. 423-444
- [15] Ahuja, A. S., Augmentation of Heat Transport in Laminar Flow of Polystyrene Suspension: Experiments and Results, *Journal of Applied Physics*, 46 (1975), 8, pp. 3408-3416
- [16] Karimi, A., *et al.*, Experimental Studies on the Viscosity of Fe Nanoparticles Dispersed in Ethylene Glycol and Water Mixture, *Thermal Science*, 20 (2016), 5, pp. 1661-1670
- [17] Sundar, S. L., Manoj, K., Convective Heat Transfer and Friction Factor Correlations of Nanofluid in a Tube and with Inserts: A review, *Renewable and Sustainable Energy Reviews*, 20 (2013), Apr., pp. 23-35
- [18] Chandrasekar, M., *et al.*, Experimental Studies on Heat Transfer and Friction Factor Characteristics of Al₂O₃-Water Nanofluid in a Circular Pipe under Transition Flow with Wire Coil Inserts, *Heat Transfer Engineering*, 32 (2011), 6, pp. 485-496
- [19] Selvaraj, P., *et al.*, Computational Fluid Dynamics Analysis on Heat Transfer and Friction Factor Characteristics of a Turbulent Flow for Internally Grooved Tubes, *Thermal Science*, 17 (2013), 4, pp. 1125-1137
- [20] Selvam, S., *et al.*, Experimental Studies on Effect of Bonding the Twisted Tape with Pins to the Inner Surface of the Circular Tube, *Thermal Science*, 18 (2014), 4, pp. 1273-1283
- [21] Suresh, S., *et al.*, Experimental Studies on Heat Transfer and Friction Factor Characteristics of Al₂O₃/Water Nanofluid under Turbulent Flow with Spiraled Rod Inserts, *Chemical Engineering and Processing*, 53 (2012), Mar., pp. 24-30
- [22] Chandrasekar, M., *et al.*, Experimental Studies on Heat Transfer and Friction Factor Characteristics of Al₂O₃/Water Nanofluid in a Circular Pipe under Laminar Flow with Wire Coil Inserts, *Experimental Thermal and Fluid Science*, 34 (2010), 2, pp. 122-130
- [23] Shahidi, M., *et al.*, Experimental and Numerical Investigation on Turbulent Flow of Mwcnt-Water Nanofluid inside Vertical Coiled Wire Inserted Tubes, *Thermal Science*, On-line first, <https://doi.org/10.2298/TSCI151025069S>
- [24] Turgut, I., *et al.*, Thermal Conductivity and Viscosity Measurements of Water-Based TiO₂ Nanofluids, *Int J Thermophys*, 30 (2009), 4, pp. 1213-1226
- [25] Kumar, D. H., *et al.*, Model for Heat Conduction in Nanofluids, *Physical Review Letters*, 93 (2004), Sept., 144301
- [26] Yu, W., Choi, S. U. S., The Role of Interfacial Layers in the Enhanced Thermal Conductivity of Nanofluids: A Renovated Maxwell Model, *Journal of Nanoparticle Research*, 5 (2003), 1-2, pp. 167-171
- [27] Murshed, S. M. S., *et al.*, Thermal Conductivity of Nanoparticle Suspensions (Nanofluids), *Proceedings, IEEE Conference on Emerging Technologies-Nanoelectronics*, Singapore, 2006, pp. 155-158
- [28] Wei, Y., Huaqing, X., A Review on Nanofluids: Preparation, Stability Mechanisms and Applications, *Journal of Nanomaterials*, 120 (2012), ID435873